Soil & Tillage Research 198 (2020) 104553

Contents lists available at ScienceDirect

Soil & Tillage Research

journal homepage: www.elsevier.com/locate/still

Anisotropy of unsaturated soil hydraulic properties of eroded Luvisol after conversion to hayfield comparing alfalfa and grass plots

Steffen Beck-Broichsitter[a,*], Horst H. Gerke[a], Martin Leue[a], Patrick J. von Jeetze[b], Rainer Horn[c]

[a] Working Group "Hydropedology", Research Area 1 "Landscape Functioning", Leibniz Centre for Agricultural Landscape Research (ZALF), Eberswalder Straße 84, 15374 Müncheberg, Germany
[b] Chair of Soil Physics, University of Bayreuth, Germany
[c] Institute of Plant Nutrition and Soil Science, Christian-Albrechts-University Kiel, Germany

ARTICLE INFO

Keywords:
Plough pan
Soil structure
Water retention
Hydraulic conductivity

ABSTRACT

The ploughing-induced compaction of the interface between topsoil and subsoil negatively affects the connectivity and continuity of the complex pore system through plough pans as artificial boundary resulting in water-logged conditions. The conversion of arable land into hayfield is an opportunity for breaking up plough pans and recovering pore networks in the long-term. The basic idea of the current study was to investigate the potential pore structure recovery effect by growing either deep-rooting alfalfa or shallow-rooting grass on former conventionally-tilled cropland. The alfalfa and grass plots located in moraine region in Northeast Germany on erosion-affected truncated Albic Luvisol, were sampled nine years after the conversion to hayfield. Undisturbed soil cores (300 cm^3) were extracted in vertical (0°) and horizontal directions (90°) from the boundary between Ap and Al-Bt- horizons (about 25 − 35 cm soil depth). The soil water retention and the hydraulic conductivity under variable-saturated conditions were determined by using a combination of methods including suction plate, pressure chamber, double membrane through-flow, and evaporation experiments. The anisotropy ratio, AR, (horizontal versus vertical) of the unsaturated hydraulic conductivity function, K(Se), was less pronounced for the soil at the alfalfa as compared to that of the grass plot, especially for wide coarse pores (wCP: > −60 hPa). The AR-ratio was differently depending on the pore size for soil from grass and alfalfa plot, and ranged between AR-values of 1 and 7. The pore size class-related matric flow potential, ϕ, derived from K(Se) function was used for comparing the volume fraction of pore size classes with a pore size-related fraction of the capillary potential. The volume fraction of the wide coarse pores was negatively related with ϕ (r^2: 0.91). The smaller AR-values for the soil of the alfalfa plot suggest a tendency for better changing the platy structure into a prismatic-platy structure through the more intense rooting in the vertical direction than in the soil of the grass plot.

1. Introduction

Ploughing is still the most common practice of breaking the soil structure to prepare it for agricultural purposes, while reducing the soil aggregate stability along with losses of soil organic matter in the topsoil (Ivelic-Sáez et al., 2015; Martínez-Casanovas and Ramos, 2009). In addition, the so-called plough pan in about 0.25–0.35 m soil depth (e.g., Herbrich and Gerke, 2017) can affect the root growth; and the nutrient accessibility for plants through limited soil aeration in a compacted plough pan (Li et al., 2019). However, the induced mechanical load through ploughing can result in a predominantly platy soil structure of the plough pan when the induced mechanical stresses exceed the stability of the soil structure measured as precompression stress (Zink et al., 2011). Compaction is affecting capacity parameters (e.g., air-filled porosity) and resulting in direction-dependent behaviour of intensity parameters (e.g., hydraulic conductivity, air permeability) through a predominantly higher pore continuity and connectivity in horizontal than in vertical direction (Reszkowska et al., 2011; Zhai and Horn, 2018; Zhang, 2014).

For the structural reclamation of a plough pan, mainly mechanical soil loosening or crop rotations are advised (e.g., Zink et al., 2011). In this case, the temporary conversion of arable land into grassland (hayfields, meadows) is a common practise in agriculture to reduce ploughing-induced long-term soil degradation effects (soil erosion, harvest losses). Therefore, predominantly shallow-rooting perennial grasses (*P. pratensis* L.) and deep-rooting plants such as alfalfa (*M. sativa* L.) reaching soil depths of up to 4.0 m were identified as useful "plough pan breakers" (Dörner et al., 2011; Fan et al., 2016). The soil structural

* Corresponding author.
E-mail address: steffen.beck-broichsitter@zalf.de (S. Beck-Broichsitter).

https://doi.org/10.1016/j.still.2019.104553
Received 16 April 2019; Received in revised form 22 November 2019; Accepted 18 December 2019

reclamation effects on hayfields and meadows can also be enhanced through an increasing quality and number of worm burrows (Soracco et al., 2015), which are improving the long-term oxygen supply of plant roots (Lipiec and Hatano, 2003; Martínez-Casanovas and Ramos, 2009).

The idea of the present study was to identify the long-term effects of differently root-intensive plant species on the soil pore structure of this critical soil region (i.e., bottom topsoil and upper subsoil). Deep rooting alfalfa is known to create continuous vertical macropores, while the shallow-rooting grass is known to form a more uniformly-distributed pore network of smaller-sized biopores in multiple directions. The initially relatively sharp boundary between Ap horizon and subsoil with horizontally-oriented pores could remain intact for differently long periods of time depending on the plant species. Anisotropy in the hydraulic conductivity (K) near the former Ap-subsoil boundary should vary depending on the pore sizes and crop type. Relatively larger vertical K-values in the macropore size range are expected for the soil at the alfalfa plot while for the soil at the grass plot, the horizontal K-values should be larger in the medium pore size range.

The authors hypothesised that (i) the pore size distribution and (ii) the unsaturated soil hydraulic properties of the critical soil horizon differ in the soil of the alfalfa plot from that of the grassland plot. These differences of the anisotropy factor are a function of the pressure head and can be identified for specific pore size fractions.

The objectives of this study were to compare the potential for plough pan breaking and soil structure formation of alfalfa and grass hayfield plots. We analysed the pore size distribution and the potential for identifying the direction-dependency of the saturated (Ks) and unsaturated hydraulic conductivity (K(Se)). For the comparison of long-term differences between the soils of the alfalfa and grass plots after a no-till period of nine years, a number of experimental laboratory methods and analytical models were employed to determine soil water retention and unsaturated hydraulic conductivity data with uni- and bimodal van Genuchten-type functions.

2. Materials and methods

2.1. Site and soil

Sampling was carried out on two soil pits in a field in the village of Krummenpfahl (52°76‘99”N, 13°92‘56”E) located about 55 km northeast of the city of Berlin and 35 km north of the Leibniz Centre for Agricultural Landscape Research (ZALF) in Müncheberg in the state of Brandenburg (Northeast Germany). The region is in a hummocky morainic post-glacial landscape and characterised by a sub-continental climate with mean annual precipitation of 550 mm and an annual average air temperature of about 9.3 °C (in 2 m) for the period between 1994 and 2018 measured at the ZALF weather station in Müncheberg (52°51’57”N, 14°11’29”E). The ground morainic arable soils are more-or-less eroded glacial till-derived Luvisols (e.g., Herbrich and Gerke, 2017). The soil profiles showed all signs of long-term tillage activities such as a clear boundary between top- and subsoil (Fig. 1a), an erosion-affected truncated Albic Luvisol profile (Ap/Ah, E and E/Bt, Btg, CBkg and elCcv horizons) according to FAO soil classification (IUSS Working Group WRB, 2015), and small-scale heterogeneous subsoil representing morainic glacial till parent material (Fig. 1b).

Here, the prismatic-platy structured lower topsoil (0.2–0.3 m depth) had a sand-dominated loamy texture (Table 1) with relatively low organic carbon contents (about 0.5 %), pH-values (5.3–5.9), and relatively high bulk densities (1.64–1.71 g cm^{-3}).

The field has been conventionally tilled and cropped before for many decades with mouldboard ploughing to a depth of about 0.25 m (Ap-horizon). In 2004, nine years before the soil sampling campaign, the formerly tilled cropland was turned into a hayfield; one part was sown with a grass mixture (mainly *P. pratensis* L., *F. rubra* L.) and the other with alfalfa (*M. sativa* L.). The grass was cut 2-times and the alfalfa 3- to 4-times a year for hay production.

Because of the erosion-affected profile truncation, the previous ploughing activities did not result in a massive plow pan below the Ap-horizon but still, a relatively compact upper subsoil horizon was created as observed in soils exposed to long-term tillage practices (e.g., Schlüter et al., 2018). After the conversion, the bulk density of the former Ap horizon increased (e.g., Kalinina et al., 2018) because of absence of cultivation while machinery traffic continued and modified soil process dynamics as reported elsewhere (Pires et al., 2017). As a result, a layer developed that combines the more recently compacted bottom topsoil and the upper subsoil that was compacted before from long-term tillage. Thus, the degree of compaction in terms of the pre-compression stress gradually increased from the topsoil downwards to values of 163 kPa for the soil at the grass plot and 146 kPa for that of the alfalfa plot, values decreased further down to 148 kPa (grass) and 98 kPa (alfalfa) in 0.5 m depth.

2.2. Soil physical and hydraulic properties

Soil texture was analysed by the combined wet sieving (> 0.063 mm) and pipette method (≤ 0.02 mm) after carbonate removal and organic carbon destruction on disturbed soil material in 4 replicates per depth (Hartge and Horn, 2016). The disturbed soil was from the direct surrounding of the intact cores that were sampled for determination of soil hydraulic properties. The bulk density and the soil water retention and unsaturated hydraulic conductivity functions were obtained from intact soil cores of 300 cm^3 (6 cm height) in 5 replicates by using a combination of methods for defined moisture ranges (Fig. 2). The procedure started with the drainage at a sand bed (applied pressure heads, h, were −5, −10, −20, −50, and −80 hPa) and the kaolin bed (−100, −200, and −300 hPa). The intact core samples were then transferred to the disc permeameter for measuring the unsaturated hydraulic conductivity during steady-state flow. The drained (−300 hPa) samples were successively wetted and equilibrated with the flux rates at −20, −10, −5, and −1 hPa. Then, after moving to the evaporation plates, samples were allowed to dry out to about −550 hPa (lower tensiometer) and −680 hPa (upper tensiometer) before moving

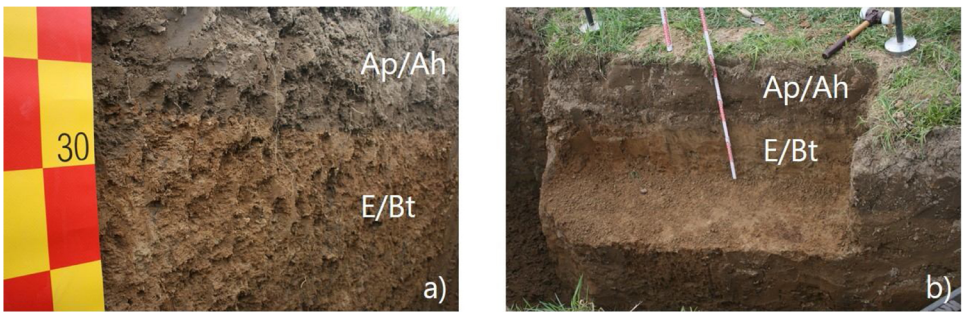

Fig. 1. Pictures of a) the boundary between topsoil and subsoil from the alfalfa plot, eroded Luvisol profile (Ap/Ah and E/Bt horizon) and b) the soil profile of the grass plot (Photos by H.H. Gerke, 2013).

Table 1
Basic soil characteristics of the alfalfa and grass plots in 0.2-0.3 m depth; organic carbon content (OC), pH ($CaCl_2$) values, soil texture, sand (2–0.063 mm), silt (0.063–0.002 mm), clay (< 0.002 mm), and dry soil bulk density (ρ_b) in vertical (ver) and horizontal (hor) sampling direction, $K(h_{-1})$ is the unsaturated hydraulic conductivity at −1 hPa; mean values and standard deviation (± symbol) from 4 replicates (5 replicates for ρ_b).

Plot		OC g kg^{-1}	pH –	Sand g kg^{-1}	Silt	Clay	ρ_b g cm^{-3}	K (h_{-1}) cm d^{-1}
alfalfa	ver	0.52 ± 0.1	5.6 ± 0.03	480 ± 15	320 ± 7	200 ± 5	1.64 ± 0.5	10.5 ± 4.1
	hor						1.71 ± 0.3	8.9 ± 4.2
grass	ver	0.35 ± 0.1	5.3 ± 0.05	470 ± 13	330 ± 9	200 ± 4	1.64 ± 0.5	9.1 ± 7.1
	hor						1.69 ± 0.3	25.5 ± 6.2

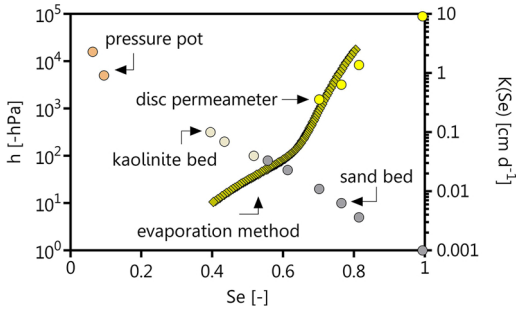

Fig. 2. Schematic description of applied measurement techniques to estimate the soil physical properties of the alfalfa and grass plot in 0.25 m depth.

them to pressure chambers to determine moisture contents at h-values of −5000 and −15,000 hPa with equilibration time of four weeks, respectively. Samples were finally oven-dried for 24 h at 105 °C (Blake and Hartge, 1986) to determine the bulk density, ρ_b (g cm^{-3}).

The soil porosity, ε, was calculated as:

$$\varepsilon = 1 - \frac{\rho_b}{\rho_s} \quad (1)$$

where ρ_s is solid particle density, here a value of 2.65 g cm^{-3} for ρ_s was assumed for the quartz-dominated loamy soil. From the measured water retention data, the soil air capacity (AC, cm^3 cm^{-3}) and the plant available soil water capacity (AWC, cm^3 cm^{-3}) were calculated as follows:

$$AC = \varepsilon - \theta_{-60\,hPa} \quad (2)$$

$$AWC = \theta_{-60\,hPa} - \theta_{-15000\,hPa} \quad (3)$$

where $\theta_{-60\ hPa}$ and $\theta_{-15,000\,hPa}$ denote the water contents at h-values of −60 hPa and −15,000 hPa.

The unsaturated soil hydraulic conductivity, K(h), was determined with two methods that cover a higher ($h > -20$ hPa) and a lower (about -680 hPa $< h < -20$ hPa) soil moisture range. In the first approach, four values of $K(h_i, i = 1, ..., 4,)$ were determined at imposed pressure heads, h_i of −1, −5, −10, and −20 hPa with a steady-state through-flow method. Identical values of h_i were imposed using a disc permeameter at the upper and the lower boundary of the soil cores of vertical length of Δz = 6 cm; because of membrane resistance effects, this pressure head was controlled by small tensiometers (0.6 cm diameter and 5 cm long ceramics) installed in 1.5 cm and 4.5 cm distances from upper boundary. For example, results from all applied methods are compared for single values of grass soil (Fig. 2).

When the tensiometer values showed a zero matric potential gradient inside the sample, flow was approaching steady state. The K-values were determined from water flux (q) readings by directly solving the Darcy equation as:

$$K(h_i) = \frac{-q_i}{\left(\frac{\Delta h_i}{\Delta z} + 1\right)} \quad (4)$$

where the pressure head gradient, Δh/Δz, is zero such that K is equal to the fluid flux density, –q, (here positive upwards). The flux rate was calculated from water volume changes determined with Mariotte's bottles for defined time intervals after steady state flow condition was established.

In the second approach, K(h) was determined with the evaporation method. The same intact soil cores (300 cm^3) were placed on a recording balance with two automatically recording pressure transducer tensiometers installed horizontally in 1.5 (lower) and 4.5 cm (upper) distance from the bottom. Water volume loss, ΔV [L^3], by evaporation was determined from mass loss, ΔM [M] assuming a unit density for water. The pressure head values in the sample at the upper, $h_u(t)$, and the lower, $h_l(t)$, tensiometers were used to calculate a mean hydraulic gradient, i_m [−], for each time interval, Δt = t2 − t1, across the vertical distance, Δz, between the tensiometers (3 cm) (Schindler, 1980) as:

$$i_m = \frac{1}{2}\left(\frac{h_u(t1) - h_l(t1)}{\Delta z} + \frac{h_u(t2) - h_l(t2)}{\Delta z}\right) - 1 \quad (5)$$

and hydraulic conductivity values were obtained by assuming a linear water content profile:

$$K(h^*) = \frac{\Delta V}{2A_{sc} \cdot \Delta t \cdot i_m} \quad (6)$$

where A_{sc} [L^2] is the cross-sectional area of the soil core (50 cm^2) and h* is the mean pressure head of the two tensiometers (i.e., $h^* = 0.5*(h_u + h_l)$) in the measurement time interval (here Δt = 10 min).

There is no fixed threshold gradient, i_m, in the wet range and the gradient varied at minimum between 0.4 and 0.7 cm cm^{-1}. The HYPROP soil hydraulic data evaluation software (Pertassek et al., 2011) was used for analyzing the measured data of the soil hydraulic properties and to obtain continuous functions for the characterization and comparison between vertical and horizontal samples of grass and alfalfa plots. The data obtained with the disc permeameter at relatively higher soil moisture range were included for description of the soil hydraulic properties in the larger pore-size range. Water retention data were fitted with both, the constraint unimodal (van Genuchten, 1980) and bimodal van Genuchten (vG) models (Durner, 1994):

$$Se(h) = \frac{\theta - \theta_r}{\theta_s - \theta_r} = \begin{cases} \sum_{i=1}^{2} w_i \left[1 + (\alpha_i h)^{n_i}\right]^{-m_i} & \text{for } h < 0 \\ 1 & \text{for } h \geq 0 \end{cases} \quad (7)$$

where Se(h) is the dimensionless effective saturation, θ is the volumetric water content (cm^3 cm^{-3}), θ_s is saturated and θ_r is residual water content (cm^3 cm^{-3}), α (cm^{-1}), n (−) and m (−), with $m = 1 - 1/n$, are empirical parameters for the two pore domains (index i), and w_i is a pore-domain weighing factor (bimodal: $w_1 = 1 - w_2$, unimodal: $w_2 = 0$). The unsaturated hydraulic conductivity K(Se) was described with the combination of the Mualem (1976) and van Genuchten (MvG) models and the bimodal retention function (Priesack and Durner, 2006):

$$K(Se) = K(h_i)\left(\sum_{i=1}^{k} w_i Se_i\right)^{\tau}\left(\frac{\sum_{i=1}^{k} w_i\alpha_i[1-(1-Se_i^{1/m_i})^{m_i}]}{\sum_{i=1}^{k} w_i\alpha_i}\right)^2 \quad (8)$$

where integer k denotes the modality of the model (i.e., k = 2 for bi-modal), w is a dimensionless weighing factor for the sub-curves of each pore domain ($0 < w_i < 1$ and $\Sigma w_i = 1$), $K(h_i)$ corresponds to the unsaturated hydraulic conductivity determined at pressure head of $i = -1$ hPa through steady-state through-flow method, and α, n, and m are the same MvG model parameters (Eq. (7)).

The $K(h_i)$ values were used for fitting at first the soil water retention functions and the derived fitting parameters, α, n, m, and K_s were then used in a second step for fitting the unsaturated hydraulic conductivity functions assuming a non-constant parameter τ that was not fixed to the value of 0.5.

The slope of the soil water retention curve (SWRC) in terms of effective saturation, ΔSe/Δh, was used to calculate the pore size distribution (PSD). According to Ding et al. (2016) and Beck-Broichsitter et al. (2018a,b), the pressure head of −10 hPa (about 9.81 cm) was assumed as boundary between the macropores and a) structural pores (wCP) and b) textural pores (nCP, MP, FP) assumed from peaks in the PSD at an equivalent pore diameter (Eq. (9)). The pore diameter for the different pore size classes were approx. calculated as follows (Hartge and Horn, 2016):

$$r_i = \frac{0.149}{|h_i|} \quad (9)$$

where r is the pore radii (cm) and h is the pressure head (cm), assuming 1 cm is proportional to −1 hPa, for the i-th pore size class: macropores ($h_1 \geq -10$ hPa), wide coarse pores ($-10 < h_2 \geq -60$ hPa), narrow coarse pores ($-60 < h_3 \geq -300$ hPa), medium pores ($-300 < h_4 \geq -15{,}000$ hPa), and fine pores ($h_5 < -15{,}000$ hPa).

Therefore, the pore sizes were classified as follows: macropores (MaP) with pore diameters of $d \geq 0.3$ mm, wide coarse pores (wCP) with $0.3 < d \geq 0.05$ mm, narrow coarse pores (nCP) with $0.05 < d \geq 0.01$ mm, medium pores (MP) with $0.01 < d \geq 0.0002$ mm, and fine pores (FP) with $d < 0.0002$ mm.

The anisotropy ratio (AR) was calculated as a function of Se instead of θ for better comparability between samples of different porosity as:

$$AR = \frac{K(Se)_{hor}}{K(Se)_{ver}} \quad (10)$$

where the subscripts ver and hor indicate K-values obtained from cores sampled in vertical and horizontal directions, respectively.

The matric flux potential, ϕ ($L^2\,T^{-1}$), is defined as the integral of the unsaturated hydraulic conductivity function, K(h) ($L\,T^{-1}$), over h, or equivalently, as the integral of soil water diffusivity, D(θ) ($L^2\,T^{-1}$), over θ ($L^3\,L^{-3}$). It was originally introduced to linearize the Richards equation based on the Kirchhoff integral transformation (e.g., Haverkamp and Vauclin, 1981; Raats, 1977). Here it is used to represent an integrated or effective value of the capillary pull per pore size class. The integration of the K(h) function (i.e., using the bimodal curves) was carried out numerically for pore size classes, i, as:

$$\phi_i = \int_{h^+}^{h^-} K(h_i)\, dh \quad (11)$$

where h^+ is the upper and h^- is the lower value of each of the five pressure head ranges representing macropores ($h_1 \geq -10$ hPa), wide coarse pores ($-10 < h_2 \geq -60$ hPa), narrow coarse pores ($-60 < h_3 \geq -300$ hPa), medium pores ($-300 < h_4 \geq -15{,}000$ hPa), and fine pores ($h_5 < -15{,}000$ hPa). An effective value of the anisotropy ratio, AR_i*, per pore size class, i, was calculated as:

$$AR_i^* = \phi_i \int_{h^+}^{h^-} \frac{1}{AR_i} \quad (12)$$

where h^+ is the upper and h^- is the lower value of each of the five pressure head ranges as mentioned above.

2.3. Statistical analyses

The statistical differences of K(Se)-values between the soils of alfalfa and grass plots was analysed with ANOVA using the variances for $p < 0.05$. Differences of the means were assessed by Tukey`s HSD test ($p < 0.05$) with a self-customized script in R (R Development Core Team, 2008). The fitting of the observed water contents, θ, and the unsaturated hydraulic conductivity, Log K(Se) ($cm\,d^{-1}$) with HYPROP was based on the second-order Akaike Information Criterion for small sample sizes (AIC_c) calculated (Hurvich and Tsai, 1989) as:

$$AIC_c = -2(\log\text{-likelihood}) + 2\,K + \frac{2k(k+1)}{(n-k-1)} \quad (13)$$

where n is the effective sample size, and k is the number of estimated parameters. Thus, the smaller the value (i.e., the larger the absolute number), the more appropriate is the model.

For evaluating the performance of the fitted model, a descriptive measure, giving the mean deviation between the fitted and observed data is the root mean square error (RMSE):

$$RMSE = \sqrt{\frac{1}{n}\sum_{i=1}^{n}(x_{sim} - x_{obs})^2} \quad (14)$$

where x_{sim} are fitted and x_{obs} observed values, here of θ and log K(Se).

3. Results

3.1. Soil porosity and water retention characteristics

The porosity, ε, of samples from alfalfa and grass plots (0.35–0.38 $cm^3\,cm^{-3}$) is relatively similar except for small differences between the vertical and horizontal samples (Table 2). The air capacity (AC) of the soil in 20 − 30 cm depth of the grass plot is higher than that of the alfalfa plot while plant available water capacity (AWC) is similar for the soil of both plots. The water contents at wilting point (WP) are higher for samples from the alfalfa plot as compared to those of the grass plot with some differences between samples taken in horizontal and vertical directions (Table 2).

The values of the Akaike Information Criterion (AIC_c) from fitting uni- and bi-modal VG soil water retention models to data are lowest for horizontal samples from the grass plot and highest for horizontal samples from alfalfa plot (Table 3).

The optimized parameters of the bimodal Mualem-van Genuchten soil hydraulic functions obtained by using HYPROP-fit (Table 4) indicate that the fraction of the second pore domain (w_2) representing the smaller pore sizes is mostly dominating (0.48–0.71).

3.2. Unsaturated hydraulic conductivity

From the double-membrane throughflow measurements, we can see significant differences in the K(h)-values at h = −1 cm between vertical samples from grass and alfalfa plots (Fig. 3), but not for the horizontal samples. At smaller pressure heads ($h \leq -5$ cm), the K(h)-

Table 2
Total soil porosity (ε), air capacity (AC) according to Eq. (3), plant available water capacity (AWC) according to Eq. (4), and water content at wilting point (WP); mean value and standard deviation (symbol ±) of 5 intact soil cores from the lower topsoil (0.2–0.3 m depth) of the two plots.

Plot		ε $cm^3\,cm^{-3}$	AC	AWC	WP
alfalfa	ver	0.38 ± 0.01	0.11 ± 0.02	0.13 ± 0.01	0.11 ± 0.01
	hor	0.35 ± 0.01	0.08 ± 0.01	0.10 ± 0.02	0.14 ± 0.01
grass	ver	0.38 ± 0.01	0.13 ± 0.02	0.13 ± 0.01	0.07 ± 0.01
	hor	0.36 ± 0.01	0.14 ± 0.03	0.11 ± 0.02	0.05 ± 0.01

Table 3
The values of the Akaike Information Criterion (AIC_c) obtained from fitting the unimodal (van Genuchten, 1980) and bimodal (Durner, 1994) soil water retention models to data of soil (0.2–0.3 m depth) from the alfalfa and grass plots sampled in vertical (ver) and horizontal (hor) direction.

AIC_c (-)				
	alfalfa		grass	
	ver	hor	ver	hor
unimodal	−71	−105	−73	−48
bimodal	−106	−111	−85	−54

values were slightly higher for horizontal than vertical samples, but differences were not significant.

From fitting the data obtained with the evaporation method to the bimodal MvG function, the soil from the alfalfa plot shows some direction-dependent differences in the soil water retention curve (SWRC) and hydraulic conductivity (K(Se)) curves (Fig. 4); the K(Se) values are slightly higher in horizontal than in vertical directions in the range of relative saturations (Se) between 0.2 and 0.6 for soil from grass plot and Se between 0.1 and 0.4 for samples from alfalfa plot.

The anisotropy in the unsaturated hydraulic conductivity in terms of larger horizontal than vertical K(Se) values for soil from grass plot was more pronounced in the medium saturation ranges (Fig. 4).

The goodness-of-fit of the bimodal MvG function to observed water content, θ, and Log K(Se) values was characterized by RMSE values between 0.003 and 0.004 $cm^3\,cm^{-3}$ and 0.09 and 0.21 $cm\,d^{-1}$, respectively (Table 5).

The anisotropy ratio (AR) calculated from the fitted MvG curves strongly differs between soils from alfalfa and grass plots (Fig. 5); for alfalfa, the AR values are nearly on the same level at larger pressure head values (around −10 hPa) and the AR peak for grass (AR > 6) is at smaller h-values of around −100 hPa. With the emptying of the macropores (h ≥ −10 hPa), higher AR values were found for soil from grass plot as compared to the alfalfa plot with AR values below 1 for medium pores (−300 < h ≥ −15,000 hPa).

The fitted pore size distributions in terms of the slope of the water retention function, ΔSe/Δh, of soils from both plots are characterised by three peaks: A structural peak between −10 and −60 hPa, a second matrix peak at about h = −100 hPa, and a third matrix peak at around h = −5000 hPa (Fig. 6).

The structural and first matrix peaks of the grass plot are comparatively higher than those of the alfalfa plot, while the direction-dependent differences were relatively small (Fig. 6).

The matric flux potential as a function of the volume fraction of the pore size classes (Fig. 7) have a negative slope for the wide coarse pores, medium pores and fine pores (linear regression with an r^2 of 0.85–0.91), a positive slope for narrow coarse pores (r^2 of 0.73) and hardly any linear relationship for the macropores (r^2 of 0.12). Despite the limited number of data points, the relations show that the number of pores in a size fraction predominantly controls the hydraulic conductivity; for the macropores the opposite seems to be true that more pores reduce the matric flux potential of that pore size class (Fig. 7).

For the ϕ-weighed anisotropy ratio, AR*, (Eq. (12)), no relationships except for the macropores (r^2 of 0.91) could be found (Fig. 7). Despite the limited number of data points, the relation indicates that the anisotropy is more pronounced the higher the number of macropores is.

4. Discussion

4.1. Soil physical characteristics: capacity parameter

The air capacities, AC, in the 0.2–0.3 m depth of both plots of > 0.05 $cm^3\,cm^{-3}$ (Table 2) are indicating that compaction was not harmful as classified by Zink et al. (2011). Still, the AC values are relatively low and may reflect problems for potential soil aeration (Reszkowska et al., 2011). However, deep-rooting alfalfa can generate sufficient soil aeration through macropores despite a low air capacity of the soil matrix (Horn and Kutilek, 2009). The mean AC values of the soil from alfalfa plot were higher for cores taken in vertical (0.11 $cm^3\,cm^{-3}$) than in horizontal direction (0.08 $cm^3\,cm^{-3}$). Since AC is a capacity parameter, these differences could not be regarded as sufficient to assume any changes in pore orientation nine years after last ploughing or for a breaking-up of the platy structure. Nevertheless, AC values indicate that the chance of capturing a larger fraction of macropores is greater during vertically- as compared to horizontally-oriented soil sampling.

4.2. Soil physical characteristics: intensity parameter

In addition to the mentioned capacity parameters above, the plough plan breaking or structure reclamation potential affecting the structure formation (platy structure → predominant prismatic-platy structure) was determined through measurements of the hydraulic conductivity in variably-saturated soils in samples taken vertically and horizontally. Therefore, several methods were combined to enable the analysis of the complete functions of soil hydraulic properties. Since the platy structure in the boundary between topsoil and subsoil as relict of the former ploughing is usually for most arable soils resulting in temporally waterlogged soils (Bertolino et al., 2010), variable-saturated hydraulic properties can be used as a site-specific identification of changes in the pore structure (Lipiec and Hatano, 2003).

The Ks-values, obtained by fitting the curves to (Se), of the soil at the alfalfa plot in 0.25 m depth (105 and 100 cm d^{-1}) and also the K(h) values of disc permeameter measurements for −1 hPa were significantly higher in vertical than in horizontal direction (Tables 1 and 4). The results can be related to the presence of macro pores (earthworm burrows) through the pronounced deep-rooting potential of alfalfa (Dörner et al., 2011) resulting in modified connectivity of vertically-oriented pore network (Uteau et al., 2013). Thus, the results indicate a more pronounced recovery of the former ploughed Luvisol in the alfalfa plot, while the compaction effects seem to be more persistent in the soil of the grass plot (K-values in Table 4) also after nine years after conversion to hayfield.

Direction-dependent differences in K(Se)-values were reported to be mostly related to the Ks values (Germer and Braun, 2015), pore size

Table 4
Parameter fits from the mean of five data points with HYPROP software of the soil water retention data with bimodal ($w_2 = 1 - w_1$) constrained ($m = 1 - n^{-1}$) van Genuchten model (Durner, 1994) and of bimodal unsaturated hydraulic conductivity K(Se) (Priesack and Durner, 2006) for alfalfa and grass plots in 0.25 m depth in vertical (ver) and horizontal (hor) sampling direction; the saturated hydraulic conductivity, Ks, and the τ –values were obtained by fitting the curves to K(Se) data.

Plot	Direction	θ_r $cm^3\,cm^{-3}$	θ_s	α_1 cm^{-1}	α_2	n_1 –	n_2	w_2 –	Ks $cm\,d^{-1}$	τ –
alfalfa	ver	0.095	0.392	0.500	0.0025	1.674	1.475	0.481	104 ± 8.3	−1.42
	hor	0.100	0.365	0.500	0.0036	1.486	1.373	0.599	100 ± 10.4	−2.21
grass	ver	0.031	0.393	0.500	0.0061	1.802	1.418	0.616	29 ± 5.1	−2.69
	hor	0.001	0.375	0.500	0.0171	2.624	1.302	0.713	31 ± 6.4	−3.23

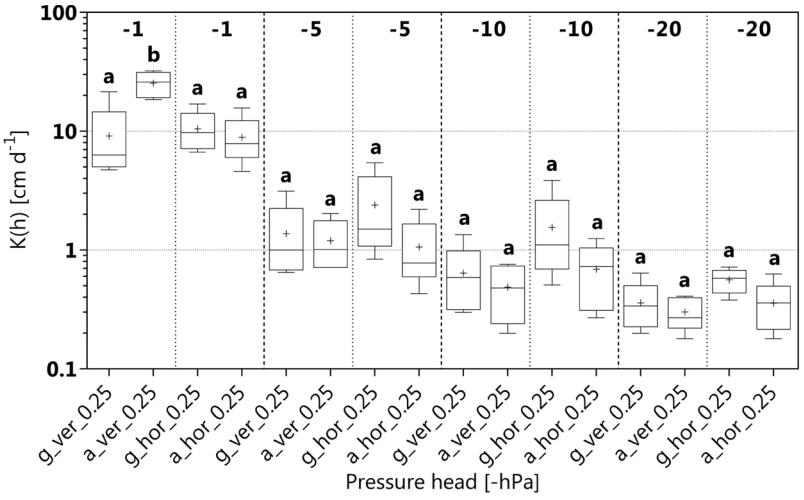

Fig. 3. Unsaturated hydraulic conductivity (K(h)) as a result of the disc permeameter measurements depending on the vegetation (alfalfa, grass), sampling direction (ver: vertical, hor: horizontal), and pressure head (−1, −5, −10, and −20 hPa). Different letters indicate differences ($p < 0.05$) in K(h) values between alfalfa and grass plot for the same direction and depth, respectively.

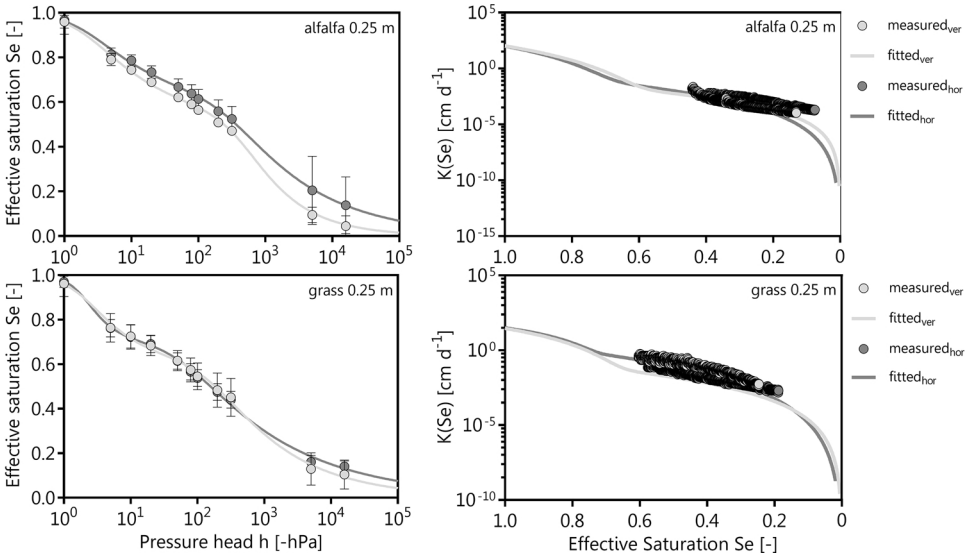

Fig. 4. Single fits from the mean of five data points with HYPROP software of the soil water retention data and unsaturated hydraulic conductivity K(Se) with bimodal van Genuchten model (Durner, 1994) and bimodal retention function (Priesack and Durner, 2006) depending on the sampling depth (0.25, m), vegetation (alfalfa, grass), and sampling direction (ver : vertical, hor: horizontal), respectively. The τ –values were obtained by fitting to K(Se) data points with $m = 1 - n^{-1}$. The error bars indicate the standard deviation at each pressure step.

Table 5
Mean deviation between the fitted and observed data in form of the root mean square error (RMSE) for water content, θ ($cm^3\,cm^{-3}$), and the unsaturated hydraulic conductivity, Log K(Se) ($cm\,d^{-1}$), based on the HYPROP software for samples from 0.25 m depth, alfalfa, grass) and sampling direction (ver: vertical, hor: horizontal).

	alfalfa		grass	
RMSE	ver	hor	ver	hor
θ	0.004	0.003	0.003	0.003
Log K(Se)	0.21	0.09	0.14	0.14

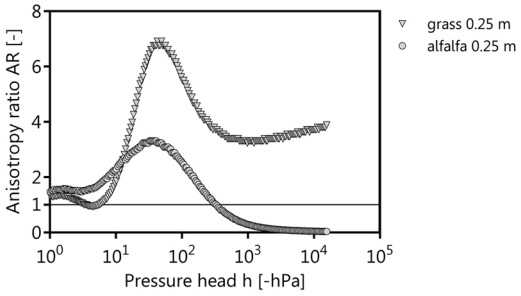

Fig. 5. Anisotropy ratio AR ($K(Se)_{hor}/K(Se)_{ver}$) as a function of the pressure head (-hPa) for 0.25 m depth and vegetation (alfalfa, grass).

distribution, and existence of macro porosity. With decreasing pressure head, the hydraulic-conductive flow cross section strongly decreasing in unsaturated soil limiting the water flow in the soil matric (Reszkowska et al., 2011). The vectors of Ks values are often assumed as isotropic, but indeed this has already been disproved (e.g., Zhai and Horn, 2018). Considering the pore size distribution (Fig. 6), the structural and matric peaks indicate the distinct decrease of K(Se) values in the coarse pore range for soils at both plots.

This is typical for sand-dominated loamy soil (sand ≥ 470 $g\,kg^{-1}$) according to Ding et al. (2016). The smooth decline in the K(Se) values for soils at the grass plot (higher VG parameter n_1) indicates a lower water capillary water absorption capacity for the coarse to medium pores which are when drained no longer able to conduct water (Alaoui et al., 2011).

Despite the limited number of data points, the K(Se) values can be related to the different pore sizes, except for macropores. This indicates that intensity parameters are functions of pore continuity and connectivity and not of capacities such as pore volume (Dörner and Horn, 2006; Zhang et al., 2006).

Considering the emptying of the wide coarse pores (wCP: > −60 hPa), the AR values for the soil at the alfalfa plot are less distinct than for the grass plot soil indicating mostly isotropic conditions (Zhang, 2014). For the soil at the grass plot, AR indicates higher

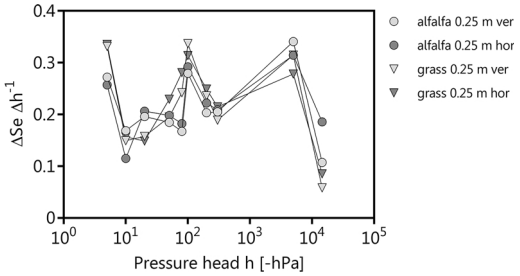

Fig. 6. Measured pore size distribution as ratio of changing pore volumes considering the slope of the soil water retention curve (ΔSe/Δh) of the alfalfa and grass plot in 0.25 m depth and vertical (ver) and horizontal (hor) directions.

horizontal than vertical K(Se) values. The relationship between the AR* (effective anisotropy ratio) and the number of macropores indicates some larger differences in the structure of soils at grass and alfalfa plots.

The nearly isotropic behaviour of Ks and K(Se) in the macropore range indicates for both plots, a tendency of breaking up the former compacted soil regions. This indicates that the previously platy structure has probably been gradually changed into a prismatic-platy structure by intense rooting and drying cycles. As an indirect proof, Uteau et al. (2013) showed that within relatively short time, alfalfa root growth significantly increased the air permeability as well as the relative gas diffusivity predominantly in vertical direction.

The ability of breaking up compacted layers was also found for sunflower (*H. annuus*), Johnson grass (*S. bicolor*), pearl millet (*P. americanum* L.) due to larger root diameters of up to 4 cm and sufficient penetration strength (Rosolem et al., 2002); alfalfa (*M. sativa*) can also add nutrients to soil through biological nitrogen fixation improving physiological activity and root growth in compacted layers (Lipiec and Hatano, 2003).

4.3. Measurement and fitting uncertainties

The AIC_c values in Table 3 indicated the lowest values for the bimodal van Genuchten model (Durner, 1994) considering that the "best" model of the given models was chosen, even though more precise potentially exist for the selected data set. The structured soils of this study can thus be assumed to have a bimodal pore structure. The RMSE values are all close to the measurement errors of 0.16 to 0.27 cm d^{-1} for the log K(Se) data (Peters and Durner, 2008), and the fitted curves can explain the observed data.

5. Conclusions

The results indicate a more distinct anisotropic behaviour for the soil of the grass plot in the range of wide to narrow coarse pores. This can be attributed to a more pronounced horizontal versus vertical matric flux potential relation for the grass as compared to the alfalfa plot. The distinct "narrowing" of direction-dependent pore size

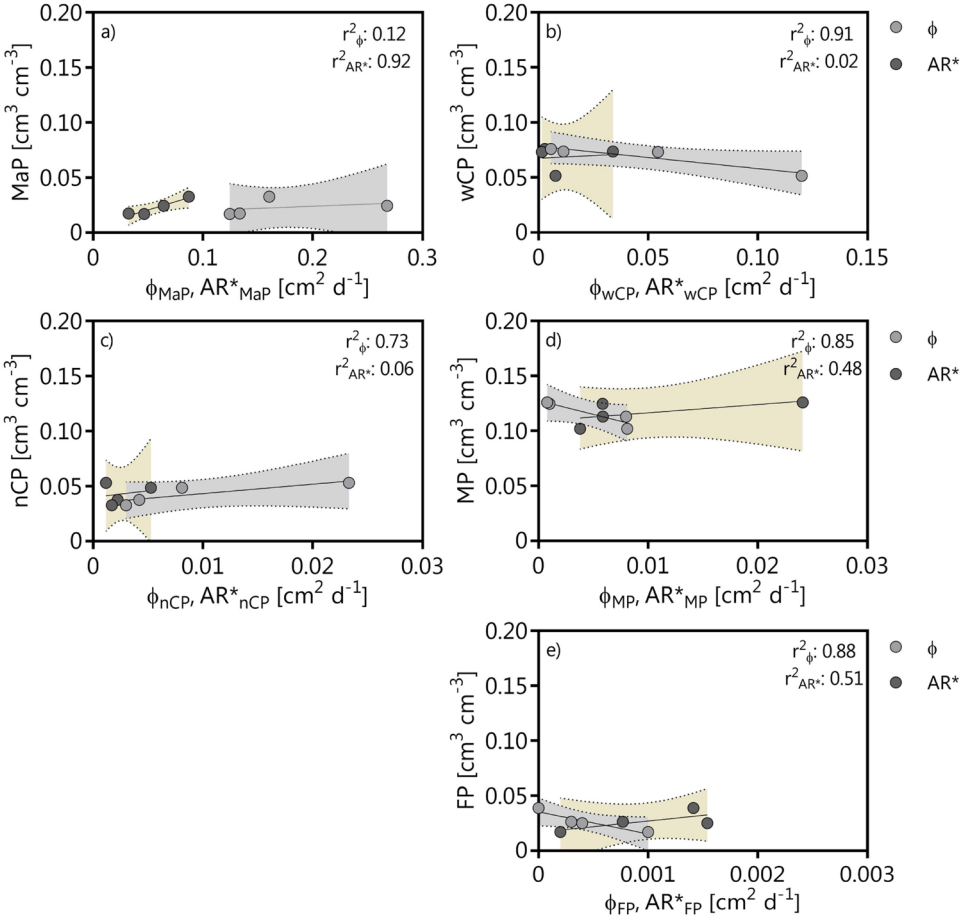

Fig. 7. Mean values of volume fraction of pore sizes versus matric flow potential (ϕ) and ϕ-weighed anisotropy ratio, AR*, for macropores (MaP) with $d \geq 0.3$ mm, wide coarse pores (wCP) with $0.3 < d \geq 0.05$ mm, narrow coarse pores (nCP) with $0.05 < d \geq 0.01$ mm, medium pores (MP) with $0.01 < d \geq 0.0002$ mm, and fine pores (FP) with $d < 0.0002$ mm. The dashed line indicates the confidence intervals (CI: 95 %) between the ϕ values and the ϕ-weighed anisotropy ratio (AR*) and the pore size distribution (pore size) and the for 8 data points, respectively.

distributions confirm the hypothesis that the recovery of the continuous pore network in vertical direction is more effective for the soil of the alfalfa plot than for the soil of the grass plot. Nevertheless, both plots underwent structural improvements. The differences between the two plots are relatively small and mainly characterized by the macro-porosity and the anisotropy - pressure head relations. Smaller AR-values for the soil of the alfalfa plot suggest a tendency for better restructuring of the ploughing-induced soil compaction as compared to the grass plot, 9-years after conversion to hayfield.

Declaration of Competing Interest

The authors declare that there is no conflict of interest.

Acknowledgements

We thank Sebastian Pagenkämper from Kiel, Martin Schmidt and Norbert Wypler from ZALF, Müncheberg, for their strong support during the soil sampling in the field. Norbert Wypler also carried out soil hydraulic laboratory measurements on core samples; his help is gratefully acknowledged. We also thank two anonymous reviewers and the Editor, Ole Wendroth, for constructive comments that helped improving the manuscript.

References

Alaoui, A., Lipiec, J., Gerke, H.H., 2011. A review of the changes in the soil pore system due to soil deformation: a hydrodynamic perspective. Soil Tillage Res. 115–116, 1–15. https://doi.org/10.1016/j.still.2011.06.002.

Beck-Broichsitter, S., Gerke, H.H., Fleige, H., Horn, R., 2018a. Effect of compaction on soil physical properties of differently textured landfill liner materials. Geosciences 9 (1). https://doi.org/10.3390/geosciences9010001.

Beck-Broichsitter, S., Gerke, H.H., Horn, R., 2018b. Shrinkage characteristics of boulder marl as sustainable mineral liner material for landfill capping systems. Sustainability 10, 4025. https://doi.org/10.3390/su10114025.

Bertolino, A.V.F.A., Fernandes, N.F., Miranda, J.P.L., Souza, A.P., Lopes, M.R.S., Palmieri, F., 2010. Effects of plough pan development on surface hydrology and on soil physical properties in Southeastern Brazilian plateau. J. Hydrol. 393, 94–104. https://doi.org/10.1016/j.jhydrol.2010.07.038.

Blake, G.R., Hartge, K.H., 1986. Bulk density. In: Klute, A. (Ed.), Methods of Soil Analysis, Part., 2nd ed. ASA and SSSA, Madison, WI, USA, pp. 363–375.

Ding, D., Zhao, Y., Feng, H., Peng, X., Si, B., 2016. Using the double-exponential water retention equation to determine how soil pore-size distribution is linked to soil texture. Soil Tillage Res. 156, 119–130. https://doi.org/10.1016/j.still.2015.10.007.

Dörner, J., Horn, R., 2006. Anisotropy of pore functions in structured Stagnic Luvisols in the Weichselian moraine region in N Germany. J. Plant Nutr. Soil Sci. 169, 213–220. https://doi.org/10.1002/jpln.200521844.

Dörner, J., Dec, D., Zúñiga, F., Sandoval, P., Horn, R., 2011. Effect of the land use change on Andosol's pore functions and their functional resilience after mechanical and hydraulic stresses. Soil Tillage Res. 115–116, 71–79. https://doi.org/10.1016/j.still.2011.07.002.

Durner, W., 1994. Hydraulic conductivity estimation for soils with heterogeneous pore structure. Water Resour. Res. 26, 1483–1496. https://doi.org/10.1029/93WR02676.

Fan, J., McConkey, B., Wang, H., Janzen, H., 2016. Root distribution by depth for temperature agricultural crops. Field Crops Res. 189, 68–74. https://doi.org/10.1016/j.fcr.2016.02.013.

IUSS Working Group WRB, 2015. World Reference Base for Soil Resources 2014 (Update 2015): International Soil Classification System for Naming Soils and Creating Legends for Soil Maps. World Soil Resour. Rep. 103. FAO, Rome.

Germer, K., Braun, J., 2015. Determination of anisotropic saturated hydraulic conductivity of a macroporous slope soil. Soil Sci. Soc. Am. J. 79, 1528–1536. https://doi.org/10.2136/sssaj2015.02.0071.

Hartge, K.H., Horn, R., 2016. Essential soil physics. In: Horton, R., Horn, R., Bachmann, J., Peth, S. (Eds.), An Introduction to Soil Processes, Structure, and Mechanics. Schweizerbart Science Publishers, Stuttgart, Germany, pp. 391.

Haverkamp, R., Vauclin, M., 1981. A comparative study of three forms of the Richard equation used for predicting onedimension infiltration in unsaturated soil. Soil Sci. Soc. Am. J. 45, 13–20.

Herbrich, M., Gerke, H.H., 2017. Scales of water retention dynamics observed in eroded Luvisols from an arable postglacial soil landscape. Vadose Zone J. 16 (10). https://doi.org/10.2136/vzj2017.01.0003.

Horn, R., Kutilek, M., 2009. The intensity-capacity concept—how far is it possible to predict intensity values with capacity parameters. Soil Tillage Res. 103, 1–3. https://doi.org/10.1016/j.still.2008.10.007.

Hurvich, C.M., Tsai, C.-L., 1989. Regression and time series model selection in small sample. Biometrika 76 (2), 99–104.

Ivelic-Sáez, J., Zúñiga, F., Valle, S., López, I., Dec, D., Dörner, J., 2015. Functional resistance and resilience of the pore system of an Andisol exposed to different strategies of pasture improvement under sheep grazing. J. Soil Sci. Plant Nutr. 15 (3), 663–679. https://doi.org/10.4067/S0718-95162015005000045.

Kalinina, O., Chertov, O., Frolov, P., Goryachkin, S., Kuner, P., Küper, J., Kurganova, I., Lopes de Gerenyu, V., Lyuri, D., Rusakov, A., Kuzyakov, Y., Giani, L., 2018. Alteration process during the post-agricultural restoration of Luvisols of the temperate broad-leaved forest in Russia. Catena 171, 602–612. https://doi.org/10.1016/j.catena.2018.08.004.

Li, Y., Zhai, Z., Cong, P., Zhang, Y., Pang, H., Dong, G., Gao, J., 2019. Effect of plough pan thickness on crop growth parameters, nitrogen uptake and greenhouse gas ($CO_2$and N_2O) emissions in a wheat-maize double-crop rotation in the Northern China Plain: a one-year study. Agric. Water Manag. 213, 534–545. https://doi.org/10.1016/j.agwat.2018.10.044.

Lipiec, J., Hatano, R., 2003. Quantification of compaction effects on soil physical properties and crop growth. Geoderma 116 (1–2), 107–136. https://doi.org/10.1016/S0016-7061(03)00097-1.

Martínez-Casanovas, J.A., Ramos, M.C., 2009. Soil alteration due to erosion, ploughing and levelling of vineyards in north east Spain. Soil Use Manage. 25 (2), 183–192. https://doi.org/10.1111/j.1475-2743.2009.00215.

Mualem, Y., 1976. A new model predicting the hydraulic conductivity of unsaturated porous media. Water Resour. Res. 12, 513–522.

Pertassek, T., Peters, A., Durner, W., 2011. HYPROP Data Evaluation Software User's Manual, V.1.0. UMS GmbH, Gmunder Str. 37, 81379 München, Germany.

Peters, A., Durner, W., 2008. A simple model for describing hydraulic conductivity in unsaturated porous media accounting for film and capillary flow. Water Resour. Res. 44. https://doi.org/10.1029/2008WR007136.

Pires, L.F., Borges, J.A.R., Rosa, J.A., Cooper, M., Heck, R.J., Passoni, S., Roque, W.L., 2017. Soil structure changes induced by tillage systems. Soil Tillage Res. 165, 66–79.

Priesack, E., Durner, W., 2006. Closed-form expression for the multi-modal unsaturated hydraulic conductivity. Vadose Zone J. 5, 121–124. https://doi.org/10.2136/vzj2005.0066.

R Development Core Team, 2008. R: A Language and Environment for Statistical Computing. R Foundation for Statistical Computing, Vienna, Austria.

Raats, P.A.C., 1977. Laterally confined, steady flows of water from sources and to sinks in unsaturated soils. Soil Sci. Soc. Am. J. 41 (2), 294–304.

Reszkowska, A., Krümmelbein, J., Peth, S., Horn, R., Zhao, Y., Gan, L., 2011. Influence of grazing on hydraulic and mechanical properties of semiarid steppe soils under different vegetation type in Inner Mongolia, China. Plant Soil 340, 59–72. https://doi.org/10.1007/s11104-010-0405-3.

Rosolem, C., Foloni, J., Tiritan, C., 2002. Root growth and nutrient accumulation in cover crops as affected by soil compaction. Soil Tillage Res. 65, 109–115. https://doi.org/10.1016/S0167-1987(01)00286-0.

Schindler, U., 1980. Ein Schnellverfahren zur Messung der Wasserleitfähigkeit im teilgesättigten Boden an Stechzylinderproben. Arch. Acker Pflanzenbau Bodenkd 24, 1–7.

Schlüter, S., Großmann, C., Diel, J., Wu, G.-M., Tischer, S., Deubel, A., Rücknagel, J., 2018. Long-term effects of conventional and reduced tillage on soil structure, soil ecological and soil hydraulic properties. Geoderma 332, 10–19. https://doi.org/10.1016/j.geoderma.2018.07.001.

Soracco, C.G., Lozano, L.A., Villarreal, R., Palancar, T.C., Collazo, D.J., Sarli, G.O., Filgueira, R.R., 2015. Effects of compaction due to machinery traffic on soil pore configuration. Rev. Bras. Ciênc. Solo 39, 408–415. https://doi.org/10.1590/01000683rbcs20140359.

Uteau, D., Pagenkemper, S.K., Peth, S., Horn, R., 2013. Root and time dependent soil structure formation and its influence on gas transport in the subsoil. Soil Tillage Res. 132, 69–76. https://doi.org/10.1016/j.still.2013.05.001.

van Genuchten, M.T., 1980. A closed-form equation for predicting the hydraulic conductivity of unsaturated soils. Soil Sci. Soc. Am. J. 44, 892–898.

Zhang, S.L., Grip, H., Lovdahl, L., 2006. Effect of soil compaction on hydraulic properties of two loess soils in China. Soil Tillage Res. 90 (1–2), 117–125. https://doi.org/10.1016/j.still.2005.08.012.

Zhang, Z.F., 2014. Relationship between anisotropy in soil hydraulic conductivity and saturation. Vadose Zone J. 13 (6). https://doi.org/10.2136/vzj2013.09.0172.

Zhai, X., Horn, R., 2018. Effect of static and cyclic loading including spatial variation caused by vertical holes on changes in soil aeration. Soil Tillage Res. 177, 61–67. https://doi.org/10.1016/j.still.2017.11.008016/.

Zink, A., Fleige, H., Horn, R., 2011. Verification of harmful subsoil compaction in loess soils. Soil Tillage Res. 114, 127–134. https://doi.org/10.1016/j.still.2011.04.004.